

Redesign and Analysis of Globally Asymptotically Stable Bearing Only SLAM

Elias Bjørne* Tor Arne Johansen* Edmund Førland Brekke*

Abstract—The Simultaneous Localization And Mapping (SLAM) estimation problem is a nonlinear problem, due to the nature of the range and bearing measurements. In latter years it has been demonstrated that if the nonlinearities from the attitude are handled by a separate nonlinear observer, the SLAM dynamics can be represented as a linear time varying (LTV) system, by introducing these nonlinearities and nonlinear measurements as time varying vectors and matrices. This makes the SLAM estimation problem globally solvable with a Kalman filter, however, the noise structure is no longer trivial. In this paper, a new bearings only SLAM estimation algorithm is presented, including a novel design of the noise covariance matrices. Simulations of the SLAM estimator are presented, and show the performance of the state and uncertainty estimates, as well as the stability of the proposed estimator.

Index Terms—Navigation, Sensor data fusion, Localisation, Mapping, Kalman Filter

I. INTRODUCTION

Robust navigation and positioning of unmanned aerial vehicles (UAVs) are fundamental for any autonomous mission, particularly in challenging environments where absolute positioning systems are absent or unreliable. A scenario where the UAV's and other autonomous vehicles are used for inspection missions, demonstrates the need of high accuracy and consistency in position and attitude estimates. In this scenario the vehicles will have to work as closely as possible to the inspection target, which increases the need for stable, consistent and accurate estimates. Missions can be the inspection of structures such as bridges, power lines, windmills etc. In this case, the electromagnetic interference and the existence of ferromagnetic materials from the environment may degrade any magnetometer to the point of becoming unusable [1]. To tackle these situations, aided navigation techniques such as simultaneous localization and mapping algorithm (SLAM) can be used. SLAM fuses the data from the surroundings with the data from the inertial measurements unit (IMU) to increase accuracy in the navigation. By assuming stationary landmarks, the change in the landmarks relative positions (LRP) can give information about the motion of the vessel, and hence can be fused with the IMU to increase navigation estimates. These sensors are typically provided in ranges and/or bearing angles between the vehicle

and each landmark, and with these SLAM also builds a map of the surroundings of the vehicle. Over the past decades, the research community has devoted tremendous effort in the field of probabilistic SLAM. For a detailed review on SLAM see [2] and [3], and the references within, which includes several successful implementations of SLAM algorithms in experiments. A common approach is to use the extended Kalman filter (EKF) SLAM, however, there are some challenges related to consistency and stability, especially in regards of the error in the linearization due to wrong attitude estimates [4]. For bearing only SLAM, there are a variety of methods; filter banks [5], Rao-Blackwellized particle filters (RBPF)[6], linear mono SLAM [7] and multi-state constraint Kalman filter (MSCKF) [8]. In [9], a hybridized SLAM decides if a feature is processed using MSCKF or EKF, depending on the feature's track length; this in order to decrease computation time.

A proposed structure for global exponentially stable (GES) estimation was presented by Johansen and Brekke [10], for range and bearing, bearing only and range only SLAM. Nonlinearities from the attitude are handled by a nonlinear observer [11], so that the the nonlinear system can be represented as a linear time varying (LTV) system. This gives the LTV system

$$\dot{x}(t) = A(z(t), t)x(t) + B(z(t), t)u(t) \quad (1)$$

$$y(t) = C(z(t), t)x(t) \quad (2)$$

where x is a vector with the states of the vehicle and landmark positions, y is the vector output with a linear time varying dependency to the states. The vector z contains auxiliary, possibly nonlinear, measurements, such as attitude and bearing angles represented as a linear time varying rotation matrix and line of sight (LOS) vectors; The u are the inputs to the system such as acceleration. This representation makes the SLAM problem solvable with the Kalman filter (KF), and global stability can be proven by observability analysis [12]. Further, necessary and sufficient conditions on the observability of the nonlinear system are derived in [13]. Similar work, is done by Lourenco and Guerreiro [14][1], in which a globally asymptotically stable (GAS) sensor-based SLAM estimation is presented, for range and bearing, bearing only and range only measurements. In addition, they are able to estimate the gyro bias with range and bearing measurements. They also present the SLAM problem as a LTV system and uses KF for estimation, however, they present the system in the coordinate system of the sensors, called robosentric coordinate system.

Elias Bjørne*, Edmund Førland Brekke* and Tor Arne Johansen* are with the Centre for Autonomous Marine Operations and Systems and Department of Engineering Cybernetics, Norwegian University of Science and Technology (NTNU), NO-7491 Trondheim, Norway. (Email: elias.bjorne@itk.ntnu.no, tor.arne.johansen@itk.ntnu.no)

A. Contribution

The contribution of this paper is two-folded. The main contribution is the redesign of the bearing only SLAM presented in [10]. The new design requires less sensors as it uses neither gyro nor bearing derivative. In addition, an intuitive assumption for achieving observability is found, and is less restrictive compared to the one from [10], explained in Section III. In addition, a novel design of the output covariance matrices through linearisation are proposed and analysed. Simulations are done in 2D, and Monte Carlo (MC) simulations were used to investigate the consistency of the SLAM estimator.

The structure of this paper is as follows: Notation and preliminaries are presented in Section II; Section III contains the previous work of the presented SLAM estimation; Section IV presents the new bearing only SLAM estimation, with observability analysis of the system. Section V presents the design of the covariance matrix, while Section VI shows the simulation results. Section VII concludes the paper and suggests future work.

II. NOTATION AND PRELIMINARIES

A. Notation and math

Scalars are in lower case a, x, ω , vectors are lower case bold $\mathbf{a}, \mathbf{x}, \boldsymbol{\omega}$, matrices are bold upper case $\mathbf{A}, \mathbf{X}, \boldsymbol{\Omega}$, and sets are upper case A, X, Ω . Exceptions may happen. The 0 denotes the scalar zero, while $\mathbf{0}$ is the matrix zero where dimensions are implicitly given by the context. The accents $\hat{\bullet}, \tilde{\bullet}, \dot{\bullet}, \bar{\bullet}$, denotes estimate, estimate error, time derivative and upper bound. Random white noise variables are denoted w_{\bullet} for scalars and \mathbf{w}_{\bullet} for vectors. The subscript \bullet_m denotes the measured value. Some common mathematical expressions are: The Euclidean norm for vectors denoted $\|\bullet\|$, absolute value, denoted $|\bullet|$ and the transpose, denoted \bullet^{\top} . The representation of index sets will be done with $\{1, n\} = \{x \in \mathbb{Z} | x \leq n\}$.

A vector can be represented in different coordinate systems, the representation is denoted with the superscripts \bullet^b, \bullet^n which represents the body-fixed and inertia-fixed coordinate systems, and will be called body-frame and inertia-frame. Lower case will denote the indices of a landmark, vector or matrix \bullet_i and \bullet_{ij} .

B. Rotation

Rotation is the attitude change between two coordinate systems, and a rotation from coordinate system b to n is denoted with subscript \bullet_{nb} . This can be represented as:

Euler angles

$\boldsymbol{\theta}_{nb} = [\rho, \phi, \psi]^{\top} \in \{\mathbb{R}^3 | |\rho| \leq \pi, |\phi| \leq \pi, |\psi| \leq \pi\}$, or rotation matrix

$\mathcal{R}_{nb} \in SO(3)$

where $SO(3) = \{\mathcal{R}_{nb} \in \mathbb{R}^{3 \times 3} | \mathcal{R}_{nb}^{\top} \mathcal{R}_{nb} = \mathbf{I}, \det(\mathcal{R}_{nb}) = 1\}$. The rotation of vector \mathbf{x}^b is calculated with the rotation matrix $\mathbf{x}^n = \mathcal{R}_{nb} \mathbf{x}^b$. The cross product is presented in

matrix form as $S(\mathbf{x})\mathbf{y} = \mathbf{x} \times \mathbf{y}$, where $S(\bullet)$ is a skew-symmetric matrix

$$\mathbf{S}(\mathbf{x}) = \begin{bmatrix} 0 & -x_3 & x_2 \\ x_3 & 0 & -x_1 \\ -x_2 & x_1 & 0 \end{bmatrix} \text{ or } \mathbf{S}(x) = \begin{bmatrix} 0 & -x \\ x & 0 \end{bmatrix} \quad (3)$$

where for two dimensions the \mathbf{S} matrix corresponds to the cross product $[0, 0, x] \times [y_1, y_2, 0]$. Here x could represent rotation rate ω for instance in a 2-D scenario. More detailed information can be found in Sola [15] and Fossen [16]. Let the rotation matrix denote the rotation from the body-fixed frame to an inertia-fixed frame. The attitude dynamics is described by

$$\dot{\mathcal{R}}_{nb} = \mathcal{R}_{nb} \mathbf{S}(\boldsymbol{\omega}) \quad (4)$$

,where $\boldsymbol{\omega} = \boldsymbol{\omega}_{ib}^b$ is the angular velocity of the frame b relative to n decomposed in b . The $\boldsymbol{\omega}$ is assumed bounded $\|\boldsymbol{\omega}\| \leq \bar{\omega}$

C. Landmark and vehicle dynamics

We assume that there is a vehicle with position \mathbf{p}^n and m stationary landmarks where the i th landmark has position \mathbf{p}_i^n . The landmark relative position (LRP) are the vectors between the vehicle and the landmarks $\boldsymbol{\delta}_i^n = \mathbf{p}_i^n - \mathbf{p}^n$. This vector can be represented by its range and bearing,

$$\rho_i = \|\boldsymbol{\delta}_i^n\|, \quad l_i^n = \boldsymbol{\delta}_i^n / \|\boldsymbol{\delta}_i^n\|. \quad (5)$$

The range is the geometric distance, while the bearing is represented by a line of sight (LOS) vector on the unit ball, pointing at the landmark. These can also be presented in body-frame

$$\boldsymbol{\delta}_i^b = \mathcal{R}_{nb}^{\top} \boldsymbol{\delta}_i^n, \quad l_i^b = \mathcal{R}_{nb}^{\top} l_i^n \quad (6)$$

The kinematics of the position of the vehicle is

$$\dot{\mathbf{p}}^n = \mathbf{v}^n = \mathcal{R}_{nb} \mathbf{v}^b \quad (7)$$

and we have

$$\dot{\mathbf{v}}^n = \mathbf{f}^n + \mathbf{g}^n = \mathcal{R}_{nb} \mathbf{f}_{IMU}^b + \mathbf{g}^n \quad (8)$$

The change in the LRP is then

$$\dot{\boldsymbol{\delta}}_i^n = -\mathbf{v}^n \quad (9)$$

To find the dynamics of the LRP in body-frame, (4) and (6)-(9) were used with the product rule.

$$\dot{\boldsymbol{\delta}}_i^b = -S(\boldsymbol{\omega}) \boldsymbol{\delta}_i^b - \mathbf{v}^b \quad (10)$$

From this, the dynamics of the range and bearing can be found

$$\dot{\rho}_i = -(\mathbf{l}_i^n)^{\top} \mathbf{v}^n = -(\mathbf{l}_i^b)^{\top} \mathbf{v}^b \quad (11)$$

$$\dot{l}_i^n = \frac{1}{\rho_i} (\mathbf{l}_i^n (\mathbf{l}_i^n)^{\top} - \mathbf{I}) \mathbf{v}^n = \frac{1}{\rho_i} S(\mathbf{l}_i^n)^2 \mathbf{v}^n \quad (12)$$

$$\begin{aligned} \dot{l}_i^b &= -S(\boldsymbol{\omega}) \mathbf{l}_i^b + \frac{1}{\rho_i} (\mathbf{l}_i^b (\mathbf{l}_i^b)^{\top} - \mathbf{I}) \mathbf{v}^b \\ &= -S(\boldsymbol{\omega}) \mathbf{l}_i^b + \frac{1}{\rho_i} S(\mathbf{l}_i^b)^2 \mathbf{v}^b \end{aligned} \quad (13)$$

D. Sensor model 2-D special case

There are several sensors used for SLAM, both internal and from the surroundings. In this paper we will focus on bearing only SLAM, and the design and analysis of the noise characteristic in 2-D. We will refer to the output as the vector \mathbf{y} in (18), while the sensors will refer to the actual measurements from the sensors. The sensor models are summarized in Table I. The sensor measurements are: Attitude, bearing angle, velocity and accelerometer. We will assume that an attitude and heading reference system (AHRS) [11] is available, feeding an estimate $\hat{\psi} + w_\psi$ from which the rotation matrix can be built

$$\mathbf{R}_{nb} = \begin{bmatrix} \cos(\hat{\psi} + w_\psi) & -\sin(\hat{\psi} + w_\psi) \\ \sin(\hat{\psi} + w_\psi) & \cos(\hat{\psi} + w_\psi) \end{bmatrix} \quad (14)$$

where we see that the rotation matrix is nonlinear, and produces noise that is affected by the nonlinear transformations. Other measurements are potentially the magnetometer and accelerometer. The magnetometer is handled by the AHRS system, and the accelerometer measurement is

$$\mathbf{f}_{IMU}^b = \mathbf{f}^b + (\mathbf{R}_{nb})^\top \mathbf{g}^n \quad (15)$$

where the \mathbf{g}^n is neglected in the 2-D case, and acceleration bias can be handled as in [11]. Bearing measurements from stationary landmarks are also available. The bearing measurement in 2-D is an angle, with the measurement model

$$l_{im}^b = \begin{bmatrix} \cos(\beta_i + w_{\beta_i}) \\ \sin(\beta_i + w_{\beta_i}) \end{bmatrix} \quad (16)$$

TABLE I: Overview of the measurements used in SLAM in 2-D

Measurements	
Measurements	Noise
Bearing: $l_i^b = [\cos(\beta_i + w_\beta), \sin(\beta_i + w_\beta)]^\top (1 + w_l)$	$[w_\beta, w_l]^\top = \mathcal{N}(0, \text{diag}(\sigma_\beta, \sigma_l))$
Attitude: $\mathbf{R}_{nb} \begin{bmatrix} \cos(\psi + w_\psi) & -\sin(\psi + w_\psi) \\ \sin(\psi + w_\psi) & \cos(\psi + w_\psi) \end{bmatrix}$	$w_\psi = \mathcal{N}(0, \sigma_\psi)$
Acceleration: $\mathbf{f}_{IMU}^b = \mathbf{f}^b + w_f$	$w_f = \mathcal{N}(0, \sigma_f I_2)$
Velocity: $v^b + w_v$	$w_v = \mathcal{N}(0, \sigma_v I_2)$

E. Observability theory

As mentioned, a Kalman filter can be used on a LTV systems to get a GES observer. Consider the LTV system

$$\dot{\mathbf{x}}(t) = \mathbf{A}(t)\mathbf{x}(t) + \mathbf{B}(t)\mathbf{u}(t) + \mathbf{w}_x \quad (17)$$

$$\mathbf{y}(t) = \mathbf{C}(t)\mathbf{x}(t) + \mathbf{w}_y \quad (18)$$

with the state transition matrix $\Phi(t, t_0)$ satisfying

$$\frac{d}{dt} \Phi(t, t_0) = \mathbf{A}(t)\Phi(t, t_0) \quad (19)$$

Then the observability can be characterized by the observability Gramian [17]

$$\mathbf{W}_O(t, t+T) = \int_t^{t+T} (\mathbf{C}(\tau)\Phi(\tau, t))^\top (\mathbf{C}(\tau)\Phi(\tau, t)) d\tau \quad (20)$$

If there is a $T > 0$ such that the Gramian is positive definite for any t , the system $(\mathbf{A}(t), \mathbf{C}(t))$ is Uniformly Completely Observable (UCO) [18] [19]. The KF is then,

$$\dot{\hat{\mathbf{x}}} = \mathbf{A}(t)\hat{\mathbf{x}} + \mathbf{B}(t)\mathbf{u}(t) + \mathbf{K}(\mathbf{y} - \mathbf{C}(t)\hat{\mathbf{x}}) \quad (21)$$

$$\mathbf{K} = \mathbf{P}\mathbf{C}(t)^\top \mathbf{R}(t)^{-1} \quad (22)$$

$$\dot{\mathbf{P}} = \mathbf{A}(t)\mathbf{P} + \mathbf{P}\mathbf{A}(t) + \mathbf{Q}(t) - \mathbf{P}\mathbf{C}(t)^\top \mathbf{R}(t)^{-1} \mathbf{C}(t)\mathbf{P} \quad (23)$$

where \mathbf{R} is the positive definite covariance matrix of the measurement noise \mathbf{w}_y , and \mathbf{Q} is a positive semi-definite matrix of the process noise \mathbf{w}_x . If in addition, the covariance matrix \mathbf{Q} is such that $(\mathbf{A}(t), \sqrt{\mathbf{Q}})$ is controllable, $\mathbf{P}(0)$ is symmetric positive definite, and $\mathbf{C}(t)$ is bounded, the dynamic $\tilde{\mathbf{x}}$ is globally exponentially stable, and \mathbf{P} is uniformly bounded [12]. Here we have reviewed the continuous-time KF, for convenience, and note that its discrete-time version should be used in implementations.

III. PREVIOUS WORK

As mentioned, a GES SLAM estimation was presented by [10]. Both range and bearing, bearing only and range only SLAM were presented as a LTV system, and solved with Kalman filter. The nonlinearities from the attitude are estimated with the complimentary filter [11], with semi-globally exponentially stability. The stability of the system is then proved by observability for the LTV system. Similar work has been done by Lourenco and Guerreiro [14] [1], where a range and bearing, and bearing only, SLAM filter is presented in body-frame coordinate system. The global stability is proven with an observability analysis, thus guaranteeing GES of estimator using the Kalman filter. When using the Kalman filter, an assumption is that the process and measurement noise is Gaussian and white, and can therefore be represented by the covariance matrices \mathbf{Q} and \mathbf{R} although this is not the case for the nonlinear measurements coming out of the LOS vector and rotation matrix. This means the LTV solution is not necessary optimal but the strong convergence provided by the KF, combined with approximation of the noise characteristics; results in a stable and useful estimation.

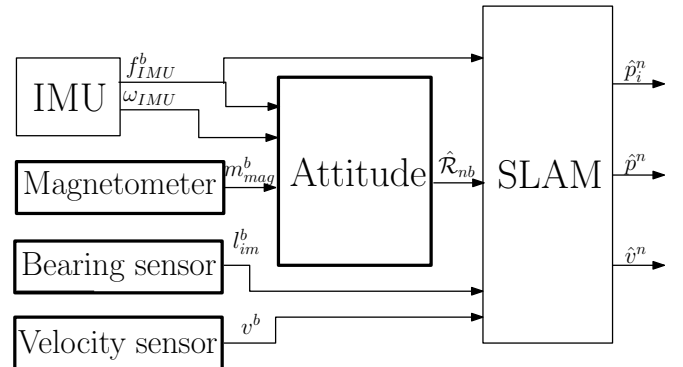


Fig. 1: Block Diagram of the structure of the SLAM attitude observer in cascade with the SLAM filter

For the observability analysis of [10], an assumption was made in which

$$\|S(\omega)l_i^b + \dot{l}_i^b\| \geq \epsilon \quad (24)$$

for some $\epsilon > 0$. By examining the dynamics of the bearing measurements (13), we see that this assumption is violated every time the velocity v^b is parallel to the bearing measurement l_i^b , which gives a restriction on the suitable paths. To address this, a new bearings only SLAM estimation is presented with a new observability analysis.

In addition, an algorithm for estimating the vehicles position was presented in [10]; where the vehicle estimate is set to zero at the start $p^n(0) = \mathbf{0}$, which gives $p_i^n = \delta_i^n(0)$. The position can then be estimated as

$$\hat{p}^n(t) = \sum_{i=1}^m w_i(t)(\delta_i^n(0) - \delta_i^n(t)) \quad (25)$$

$$\hat{p}_i^n(t) = \hat{p}^n(t) + \delta_i^n(t), \quad i = \{1, m\} \quad (26)$$

where it should be noted that the estimate will converge with a constant deviation so that $\hat{p}^n(t) = p^n(t) + d$, in which $d = \sum_{i=1}^m w_i(t)\delta_i^n(0)$.

IV. OBSERVABILITY ANALYSIS

The proposed bearing only SLAM model is presented in Table III. For the states $x = [v^n, \delta_1^n, \dots, \delta_m^n, \varrho_1, \dots, \varrho_m]^\top$, the corresponding

TABLE II: Overview of the Bearing only SLAM, for the corresponding matrices see [10]

Bearing Only SLAM, [10]	
States	Input
$x = [v^n, \delta_1^n, \dots, \delta_m^n, \varrho_1, \dots, \varrho_m]^\top$	$u = \mathcal{R}_{nb}f_{IMU}^b + g^n$
Measurement model	
$y^v = v^b = (\mathcal{R}_{nb})^\top v^n, \quad y = [y^v, y_1^V, \dots, y_m^V, y_1^E, \dots, y_m^E]^\top$	
$y_i^V = 0 = \delta_i^n - \mathcal{R}_{nb}\varrho_i l_i^b$	
$y_i^E = 0 = w_i v^n - q_i \varrho_i l_i^b$	
$w_i = S(l_i^b)^2 (\mathcal{R}_{nb})^\top, \quad q_i = S(\omega)l_i^b + \dot{l}_i^b$	
Dynamics model	
$\dot{v}^n = u$	
$\dot{\delta}_i^n = -v^n$	
$\dot{\varrho}_i = -(l_i^b)^\top (\mathcal{R}_{nb})^\top v^n$	

system matrices will be

$$\mathcal{A}^B = \begin{bmatrix} \mathbf{0} & \mathbf{0} \cdots \mathbf{0} \\ -I_3 & \mathbf{0} \cdots \mathbf{0} \\ \vdots & \ddots \vdots \\ -I_3 & \mathbf{0} \cdots \mathbf{0} \\ -(\mathcal{R}_{nb}l_1^b)^\top & \mathbf{0} \cdots \mathbf{0} \\ \vdots & \ddots \vdots \\ -(\mathcal{R}_{nb}l_m^b)^\top & \mathbf{0} \cdots \mathbf{0} \end{bmatrix} \quad \mathcal{B}^B = \begin{bmatrix} I_3 \\ \mathbf{0} \\ \vdots \\ \mathbf{0} \\ \vdots \\ \mathbf{0} \end{bmatrix}$$

$$\mathcal{C}^B = \begin{bmatrix} \mathcal{R}_{nb}^\top & \mathbf{0} & \cdots & \mathbf{0} & \mathbf{0} & \cdots & \mathbf{0} \\ \mathbf{0} & I_3 & \cdots & \mathbf{0} & -\mathcal{R}_{nb}l_1^b & \cdots & \mathbf{0} \\ \vdots & \vdots & \ddots & \vdots & \vdots & \ddots & \vdots \\ \mathbf{0} & \mathbf{0} & \cdots & I_3 & \mathbf{0} & \cdots & -\mathcal{R}_{nb}l_m^b \end{bmatrix}$$

We make an assumption on the trajectory of the vessel, to ensure observability of the bearing only SLAM:

Assumption 1: There exist a $T > 0$, so that for every landmark a $\tau_i > 0$ exists, so that for all $t > 0$ we have $t < \tau_i < t + T$, and that $l_i^n(\tau_i) \neq 0$.

This assumption ensures that the vehicle does not moves on a fixed line from a landmark (see Figure 2), ensuring that $l_i^n(\tau_i) \neq 0$ for any landmarks for the entire observation period.

Theorem 1: The model presented in Table III, is UCO if and only if assumption 1 holds.

Proof: We will use the same techniques as in [20]. In the proof we will show that the subsystems $x_i^B = [v^n, \delta_i^n, \varrho_i]^\top$ for each landmark is observable. Because of the independence of the landmarks, the entire system is completely characterized by the subsystem in terms of observability. This gives the system

$$\mathcal{A}^B(t) = \begin{bmatrix} \mathbf{0} & \mathbf{0} & \mathbf{0} \\ -I_3 & \mathbf{0} & \mathbf{0} \\ -(\mathcal{R}_{nb}(t)l_i^b(t))^\top & \mathbf{0} & \mathbf{0} \end{bmatrix}$$

$$\mathcal{C}^B = \begin{bmatrix} \mathcal{R}_{nb}^\top(t) & \mathbf{0} & \mathbf{0} \\ \mathbf{0} & I_3 & -\mathcal{R}_{nb}(t)l_i^b(t) \end{bmatrix}$$

TABLE III: Overview of proposed the Bearing only SLAM

New Bearing Only SLAM	
States	Input
$x = [v^n, \delta_1^n, \dots, \delta_m^n, \varrho_1, \dots, \varrho_m]^\top$	$u = \mathcal{R}_{nb}f_{IMU}^b + g^n$
Measurement model	
$y^v = v^b = (\mathcal{R}_{nb})^\top v^n, \quad y = [y^v, y_1^V, \dots, y_m^V]^\top$	
$y_i^V = 0 = \delta_i^n - \mathcal{R}_{nb}\varrho_i l_i^b$	
Dynamics model	
$\dot{v}^n = u$	
$\dot{\delta}_i^n = -v^n$	
$\dot{\varrho}_i = -(l_i^b)^\top (\mathcal{R}_{nb})^\top v^n$	

which is UCO as proven by calculating the transition matrix for the subsystem, and then calculating the observability Gramian. The state transition matrix is found by the Peano-Baker series [21]

$$\Phi(t, t_0) = \mathbf{I}_3 + \int_{t_0}^t \mathcal{A}^B(\sigma_1) d\sigma_1 + \int_{t_0}^t \mathcal{A}^B(\sigma_1) \int_{t_0}^{\sigma_1} \mathcal{A}^B(\sigma_2) d\sigma_2 d\sigma_1 \dots \quad (27)$$

where we see by the structure of $\mathcal{A}^B(\sigma_2)$ that $\mathcal{A}^B(\sigma_2)^2 = \mathbf{0}$, which also is the case for $\mathcal{A}^B(\sigma_1) \int_{t_0}^{\sigma_1} \mathcal{A}^B(\sigma_2) d\sigma_2 = \mathbf{0}$, because the integral preserves the zero elements of the matrix. This eliminates all the higher terms of the Peano-Baker serie, so we are left with

$$\Phi(t, t_0) = \mathbf{I}_3 + \int_{t_0}^t \mathcal{A}^B(\sigma_1) d\sigma_1 = \begin{bmatrix} \mathbf{I}_3 & \mathbf{0} & \mathbf{0} \\ (t-t_0)\mathbf{I}_3 & \mathbf{I}_3 & \mathbf{0} \\ -\mathbf{RL}_*(t, t_0)^\top & \mathbf{0} & \mathbf{I}_3 \end{bmatrix}$$

where $\mathbf{RL}_*(t, t_0) = \int_{t_0}^t \mathcal{R}_{nb}(\tau) \mathbf{l}_i^b(\tau) d\tau$. This can be inserted to (19) for confirmation. We can then calculate the observability Gramian

$$\mathcal{W}(t+T, t) = \int_t^{t+T} (\mathcal{C}^B \Phi(\tau, t))^\top (\mathcal{C}^B \Phi(\tau, t)) d\tau \quad (28)$$

$$(29)$$

where

$$\mathcal{C}^B \Phi(\tau, t) = \begin{bmatrix} \mathcal{R}_{nb}^\top & \mathbf{0} & \mathbf{0} \\ \mathbf{c}_{[1]}(\tau, t) & \mathbf{I} & \mathcal{R}_{nb} \mathbf{l}_i^b \end{bmatrix} \quad (30)$$

and $\mathbf{c}_{[1]}(t, t_0) = \mathbf{I}(t-t_0) + \mathcal{R}_{nb} \mathbf{l}_i^b \mathbf{RL}_*(t, t_0)^\top$. If the observability Gramian is full rank, the system is UCO. If $\mathcal{W}(t, t_0)$ is not full rank, there exist a vector $\mathbf{c} = [\mathbf{c}_v^\top, \mathbf{c}_\delta^\top, \mathbf{c}_\rho^\top]^\top$ with magnitude $\|\mathbf{c}\| = 1$ such that

$$\mathbf{c}^\top \mathcal{W}(t, t_0) \mathbf{c} = 0 \quad (31)$$

which corresponds to

$$\mathbf{c}^\top \mathcal{W}(t+T, t) \mathbf{c} = \int_t^{t+T} \|\mathcal{C}^B \Phi(\tau, t) \mathbf{c}\|^2 d\tau = \int_t^{t+T} \|\mathbf{f}(\tau, t)\|^2 d\tau$$

We then need to find a \mathbf{c} so that $\mathbf{f}(\tau, t) = \mathcal{C}^B \Phi(\tau, t) \mathbf{c}$ and its derivative is zero for all $\tau > 0$. Which gives the equations

$$\mathbf{f}(\tau, t) = \begin{bmatrix} \mathcal{R}_{nb}^\top(\tau) \mathbf{c}_v \\ \mathbf{c}_v \mathbf{c}_{[1]}(\tau, t) + \mathbf{c}_\delta + \mathbf{l}_i^n(\tau) \mathbf{c}_\rho \end{bmatrix} = \mathbf{0} \quad (32)$$

$$\dot{\mathbf{f}}(\tau, t_0) = \begin{bmatrix} -\mathcal{S}(\omega(\tau)) \mathcal{R}_{nb}^\top(\tau) \mathbf{c}_v \\ \mathbf{c}_v \dot{\mathbf{c}}_{[1]}(\tau, t) + \dot{\mathbf{l}}_i^n(\tau) \mathbf{c}_\rho \end{bmatrix} = \mathbf{0} \quad (33)$$

Immediately we see from (32) that it is necessary with $\mathbf{c}_v = \mathbf{0}$, which leads to the equality $\mathbf{c}_\delta = \mathbf{l}_i^n \mathbf{c}_\rho$. We also see from (33) that we need to have $\dot{\mathbf{l}}_i^n \mathbf{c}_\rho = \mathbf{0}$. By Assumption 1, there exist a τ_i such that $\dot{\mathbf{l}}_i^n(\tau_i) \neq \mathbf{0}$, which implies that we need $\mathbf{c}_\rho = \mathbf{0}$, which again imply that $\mathbf{c}_\delta = \mathbf{0}$, following from (32).

This contradicts that $\|\mathbf{c}\| = 1$. We have proven that the the Gramian $\mathcal{W}(t+T, t)$ is full rank, and the system is UCO, if and only if Assumption 1 holds. ■

In the proof we showed that the bearing only SLAM is UCO, if and only if, there exist a τ_i such that $\dot{\mathbf{l}}_i^n(\tau_i) \neq \mathbf{0}$, which implies that the inertia-frame bearing measurement $\mathcal{R}_{nb} \mathbf{l}_i^b$ can't be constant. This is shown by assuming that the bearing measurement is indeed constant, and showing that it makes the system unobservable. For the assumption $\dot{\mathbf{l}}_i^n \neq \mathbf{0}$ not to hold, we can see from (12), that the velocity vector of the vehicle has to be zero or parallel to the bearing such that $\mathcal{S}(\mathbf{l}_i^n) \mathbf{v}^n = \mathbf{0}$ for all time. By definition of observability [18], an observable system must be able to distinguish two different initial states, by the knowledge of the input and output only. Then consider the two cases, scenario *a* and *b*, where two vehicles start at different distance from a landmark, but along the same angle and moving parallel to the bearing measurements \mathbf{l}_i^n at the same velocity and orientation, and has the same acceleration (see Figure 2). This would result in them having the same matrices \mathcal{A}^B and \mathcal{C}^B . If then, they in addition start with the same estimates $[\hat{\mathbf{v}}_a^n(0), \hat{\delta}_a^n(0), \hat{\boldsymbol{\rho}}_a(0)] = [\hat{\mathbf{v}}_b^n(0), \hat{\delta}_b^n(0), \hat{\boldsymbol{\rho}}_b(0)]$, it would lead to the same state estimate evolution and output $\mathbf{y}_a(t) = \mathbf{y}_b(t)$, thus the different initial conditions are not indistinguishable from each other which makes the system unobservable. Since we have shown that the system $(\mathcal{A}^B, \mathcal{C}^B)$ is UCO if the Assumption 1 holds, we know that globally exponentially stability can be achieved for the KF in the nominal case.

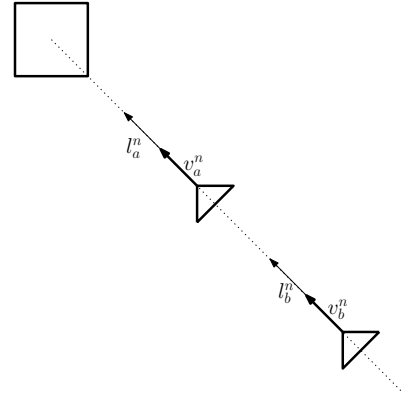


Fig. 2: Two scenarios where the vehicle starts at the same angle from a landmark, with the same velocity along parallel trajectory to its global bearing measurement.

V. COVARIANCE MATRIX DESIGN

In this section we will estimate the covariance matrices \mathbf{Q}_B and \mathbf{R}_B for the plant noise \mathbf{w}_x and output noise \mathbf{w}_y , respectively, when the bearings only SLAM is implemented. As mentioned, the dependency of \mathcal{A}^B and \mathcal{C}^B on bearing measurements and the rotation matrix, gives the need of approximating the noise characteristics. If the noises are small perturbations, linearisation can give good approximation of the noise characteristics. It should be noted that suboptimal covariance matrices \mathbf{Q}_B and \mathbf{R}_B will not damage the global

stability, which can be seen in [12]. It is shown in the proof that symmetry and positive definiteness are sufficient conditions on \mathbf{Q}_B and \mathbf{R}_B for the nominal system to be GAS. The sensor models in Section II-D for the 2-D scenario will be used.

A. Introduction of virtual noise

When approximating w_x and w_y through linearisation, a problem is that the dimension of the output vector \mathbf{y} from the bearing only SLAM in 2-D have dimension $2m + 2$, while the number of sensor measurements used in the output are $m+3$. The rank of the covariance matrix of the sensor matrix \mathbf{S}_B is therefore less than the dimension of the covariance of the output matrix \mathbf{R}_B , which can result in a singular output covariance matrix approximation

$$\hat{\mathbf{R}}_B = \mathbf{Y}_w \mathbf{S}_B \mathbf{Y}_w^\top. \quad (34)$$

The vector \mathbf{w} contains all the noise variable from the measurements, which for our case could be $\mathbf{w} = [w_{v1}, w_{v2}, w_\psi, w_{\beta1}, \dots, w_{\beta m}]^\top$. The matrix \mathbf{Y}_w is then the Jacobian $\mathbf{Y}_w = \frac{\partial \mathbf{y}}{\partial \mathbf{w}}$. With this in mind, and the fact that the distributions from the bearing vectors is nonlinear and has a covariance with dimensions two, while the bearing angle has dimension one; it is natural to introduce a virtual noise parallel to the bearing measurement

$$\mathbf{l}_{i_m}^b = \begin{bmatrix} \cos(\beta_i + w_{\beta i}) \\ \sin(\beta_i + w_{\beta i}) \end{bmatrix} (1 + w_{l_i}) \quad (35)$$

By introducing the virtual noise, the dimension of the sensor matrix increases to $2m + 3$, which ensures a full rank output covariance matrix when using (34). This also improved the performance of the filter substantially, compared to just using regularization.

B. Noise model Linearization

As mentioned, linearisation was used for approximating the nonlinear stochastic models. Hence we need the partial derivatives with regard to the noise inputs for the rotation matrix

$$\frac{\partial \mathcal{R}_{nb}}{\partial w_\psi} = \mathcal{R}_{nb} \mathbf{S}(1) \quad (36)$$

where $\mathbf{S}(1)$ is the matrix

$$\mathbf{S}(1) = \begin{bmatrix} 0 & -1 \\ 1 & 0 \end{bmatrix} \quad (37)$$

The LOS partial derivatives with regard to the noise inputs is then

$$\frac{\partial \mathbf{l}_{i_m}^b}{\partial w_{\beta j}} = \begin{cases} \mathbf{S}(1) \mathbf{l}_i^b & i = j \\ \mathbf{0} & i \neq j \end{cases} \quad (38)$$

$$\frac{\partial \mathbf{l}_{i_m}^b}{\partial w_{l_j}} = \begin{cases} \mathbf{l}_i^b & i = j \\ \mathbf{0} & i \neq j \end{cases} \quad (39)$$

Where i and j are different indices for LOS measurements. For the process model, the main noise will come from the

accelerometer, as an input to the velocity estimate $\hat{\mathbf{v}}^n$ thus propagating to the rest of the estimates by the Kalman filter. In addition, the range estimates have noise coming from the auxiliary measurement vectors \mathbf{l}_i^b and matrix \mathcal{R}_{nb} . Since these occur in both \mathbf{A}^B and \mathbf{C}^B , there will be correlations between the plant noise and the measurement noise. Simulations were done, where the noise in \mathbf{A}^B was turned off, without any notable difference, so in this paper the noise from \mathbf{A}^B and \mathbf{C}^B are assumed uncorrelated, and implemented that way. Recall that the landmark distances are given by the differential equations

$$\begin{aligned} \dot{\rho}_i &= f_i(\mathbf{x}, t) = (\mathcal{R}_{nb}(\psi_m) \mathbf{l}_i^b(\beta_m))^\top \mathbf{v}^n \\ &= (\mathcal{R}_{nb}(\psi) \mathbf{l}_i^b(\beta))^\top \mathbf{v}^n + w_{x_i} \end{aligned}$$

where w_{x_i} is the plant noise. From Table I, we see that the measurements related to \mathbf{l}_i^b and \mathcal{R}_{nb} are the attitude ψ , and bearing angles β_i . In addition, the virtual noise w_l was introduced, as explained in Section II-D. We therefore introduce the noise vector $\mathbf{w}_i = [w_\psi, w_{\beta i}, w_{l_i}]$, with covariance $\mathbf{S}_{Bi} = \text{diag}(\sigma_\psi^2, \sigma_{\beta i}^2, \sigma_{l_i}^2)$. To estimate the plant noise w_{x_i} linearisation is used

$$\hat{w}_{x_i} = \frac{\partial f_i}{\partial \mathbf{w}_i} \mathbf{w}_i = \mathbf{f}_{w_i} \mathbf{w}_i. \quad (40)$$

With partial derivatives from above we find

$$\begin{aligned} \mathbf{f}_{w_i} &= \begin{bmatrix} \frac{\partial f_i}{\partial w_\psi} & \frac{\partial f_i}{\partial w_{\beta i}} & \frac{\partial f_i}{\partial w_{l_i}} \end{bmatrix} \\ \mathbf{f}_{w_i} &= \begin{bmatrix} -(\mathcal{R}_{nb} \mathbf{S}(1) \mathbf{l}_i^b)^\top \mathbf{v}^n & -(\mathcal{R}_{nb} \mathbf{S}(1) \mathbf{l}_i^b)^\top \mathbf{v}^n & -(\mathcal{R}_{nb} \mathbf{l}_i^b)^\top \mathbf{v}^n \end{bmatrix} \end{aligned}$$

Giving the covariance of the ρ_i dynamic to be estimated as

$$\hat{\mathbf{Q}}_{B \rho_i} = \mathbf{f}_{w_i} \mathbf{S}_{Bi} \mathbf{f}_{w_i}^\top \quad (41)$$

the plant noise covariance matrix of the whole system will then become

$$\hat{\mathbf{Q}}_B = \mathbf{Q}_B + \mathbf{Q}_{Bf} + \mathbf{F}_w \mathbf{S}_B \mathbf{F}_w^\top. \quad (42)$$

The covariance matrix $\mathbf{Q}_{Bf} = \text{diag}(\sigma_f^2, \sigma_f^2, 0, \dots, 0)$ is from the accelerometer; The matrix \mathbf{Q}_B is included to allow some tuning, although it was left zero in the implementation. The matrix \mathbf{S}_B is the covariance matrix of the vector $\mathbf{w} = [w_\psi, w_{\beta 1}, w_{l_1}, \dots, w_{\beta m}, w_{l_m}]^\top$, which is the noise vector for the whole system, dependent on how many landmarks there are. The matrix \mathbf{F}_w is the Jacobian matrix with respect to the \mathbf{w} of $\dot{\mathbf{x}} = \mathbf{f}(t, \mathbf{x}) = \mathbf{A}^B \mathbf{x}$ for the whole system

$$\mathbf{F}_w = \begin{bmatrix} \mathbf{0} & \mathbf{0} & \dots & \mathbf{0} & \mathbf{f}_w^1{}^\top & \dots & \mathbf{f}_w^m{}^\top \end{bmatrix}^\top \quad (43)$$

where the row vector \mathbf{f}_w^i is the partial derivative of row number i of $\mathbf{f}(t, \mathbf{x})$ with respect of the the vector \mathbf{w} , i.e. $\mathbf{f}_w^i = [\frac{\partial f_i}{\partial w_\psi}, \dots, \frac{\partial f_i}{\partial w_{\beta i}}, \frac{\partial f_i}{\partial w_{l_i}}, \dots]$

The same method is employed for the output model. The outputs are

$$\mathbf{y}_v^B = \mathbf{g}_v(t, \mathbf{x}) = \mathcal{R}_{nb}^\top \mathbf{v}^n \quad (44)$$

$$\mathbf{y}_i^B = \mathbf{g}_i(t, \mathbf{x}) = \delta_i^b - \mathcal{R}_{nb} \mathbf{l}_i^b \rho_i \quad (45)$$

where i is the index of the landmark. To approximate the noise of the output, linearisation can also be used here

$$\hat{\mathbf{w}}_{yv} = \frac{\partial \mathbf{g}_v}{\partial \mathbf{w}_i} \mathbf{w}_i = \mathbf{G}_{wv} \mathbf{w}_i \quad (46)$$

$$\hat{\mathbf{w}}_{yi} = \frac{\partial \mathbf{g}_i}{\partial \mathbf{w}_i} \mathbf{w}_i = \mathbf{G}_{wi} \mathbf{w}_i \quad (47)$$

With partial derivatives from section II-D we find

$$\mathbf{G}_{wv} = \begin{bmatrix} \frac{\partial \mathbf{g}_v}{\partial w_\psi} & \frac{\partial \mathbf{g}_v}{\partial w_{\beta_i}} & \frac{\partial \mathbf{g}_v}{\partial w_{l_i}} \end{bmatrix}, \quad \mathbf{G}_{wi} = \begin{bmatrix} \frac{\partial \mathbf{g}_i}{\partial w_\psi} & \frac{\partial \mathbf{g}_i}{\partial w_{\beta_i}} & \frac{\partial \mathbf{g}_i}{\partial w_{l_i}} \end{bmatrix}$$

leading to

$$\mathbf{G}_{wv} = \begin{bmatrix} -\mathbf{S}(1) \mathcal{R}_{nb}^\top \mathbf{v}^n & \mathbf{0} & \mathbf{0} \end{bmatrix}$$

$$\mathbf{G}_{wi} = \begin{bmatrix} -\varrho_i \mathcal{R}_{nb} \mathbf{S}(1) \mathbf{l}_i^b & -\varrho_i \mathcal{R}_{nb} \mathbf{S}(1) \mathbf{l}_i^b & -\varrho_i \mathcal{R}_{nb} (\mathbf{l}_i^b) \end{bmatrix}$$

We can then use the same elements for the whole system, where we linearise the entire output $\mathbf{y} = \mathbf{C}^B \mathbf{x} = g(t, x) = [\mathbf{g}_v^\top, \mathbf{g}_1^\top, \dots, \mathbf{g}_m^\top]^\top$ with respect of the whole noise vector \mathbf{w} . The linearisation becomes

$$\mathbf{G}_w = \begin{bmatrix} \frac{\partial \mathbf{g}_v}{\partial w_\psi} & \mathbf{0} & \mathbf{0} & \dots & \mathbf{0} & \mathbf{0} \\ \frac{\partial \mathbf{g}_1}{\partial w_\psi} & \frac{\partial \mathbf{g}_1}{\partial w_{\beta_1}} & \frac{\partial \mathbf{g}_1}{\partial w_{l_1}} & \dots & \mathbf{0} & \mathbf{0} \\ \vdots & \vdots & \vdots & \ddots & \vdots & \vdots \\ \frac{\partial \mathbf{g}_m}{\partial w_\psi} & \mathbf{0} & \mathbf{0} & \dots & \frac{\partial \mathbf{g}_m}{\partial w_{\beta_m}} & \frac{\partial \mathbf{g}_m}{\partial w_{l_m}} \end{bmatrix}$$

We get the approximate output covariance matrix the same way we obtained the process noise covariance matrix

$$\hat{\mathbf{R}}_B = \mathbf{R}_B + \mathbf{G}_w \mathbf{S}_B \mathbf{G}_w^\top \quad (48)$$

Here, matrix \mathbf{G}_w is the Jacobian of the function $g(t, x)$, and \mathbf{S}_B is a positive definite tuning matrix, where in addition, the covariance of the velocity are maintained in the matrix elements $\mathbf{R}_{B(1:2,1:2)} = \mathbf{I} \sigma_v^2$. The matrix \mathbf{R}_B is also for tuning/regularization, ensuring that the covariance matrix is always full rank, regardless if $\hat{\varrho}_i = 0$. This was tuned so that the covariance estimates where consistent with the estimate errors.

VI. SIMULATION RESULTS AND PERFORMANCE EVALUATION

The bearings only SLAM estimator was simulated in Matlab, where the model was discretized with a time-step $\Delta t = 1[s]$ using Euler. It was implemented using the discrete-time Kalman filter, with estimates starting at the origin. The simulations are in 2D environment, and for simplicity all the landmarks are observed at all time steps. The sensors are implemented as presented in section II-D with white noise having standard deviation as follows: accelerometer $\sigma_f = 0.1[m/s^2]$, AHRS $\sigma_\psi = 0.8^\circ$, bearing angle $\sigma_\beta = 0.4^\circ$, velocity $\sigma_v = 1[m/s]$ and the virtual noise $\sigma_l = 4.5 \cdot 10^{-4}$. These were also used in the design of the covariance matrices $\hat{\mathbf{R}}_B$ and $\hat{\mathbf{Q}}_B$. The tuning/regularization matrix \mathbf{S}_B had diagonal entries $\mathbf{S}_B = \text{diag}(\sigma_v^2, 50^2, \dots, 50^2)$. The standard deviation σ_v combined with the expected initial distance to the landmarks, helped determine $\mathbf{P}(0)$. The vehicle travelled in a spiral for 1350 seconds. The results can be seen in Figure

3. The estimated vehicle trajectory and landmark estimates are in blue, while the true vehicle trajectory is in red, and the landmarks are marked with 1,2,3,4. The position estimates have also been translated, making comparison easier. The estimates converge fast, and the estimate error of landmark 1 can be seen in Figure 4. The error characteristics were the same for all the landmarks. From the error plots, it is apparent that there is a bias in the estimate error, which is oscillating. MC simulations were made for 2500 seconds, where the results of Landmark 1 are shown in Figures 5-6. In Figure 5, the average error of all the simulations is plotted for every time step. This bias vanishes if the bearing and attitude noise is turned off in the matrix \mathbf{C}_B in both filter model and simulation model. Bias compensation from Bar-Shalom [22] has been explored, without success. Nevertheless, it is apparent that the bias is predictable; and with an 1-2% error it is regarded as acceptable; which is supported by examining Figure 3. To examine the consistency of the SLAM solution, a normalized error squared (NES) test [22][p.234-236] was also preformed, resulting in Figure 6. The authors acknowledge that the NES test fails in the strictest sense, especially because of the bias. However, the result of the NES test also demonstrated stability of the solutions and the covariance estimates. So it is hardly critical, but future research should address this with more detail.

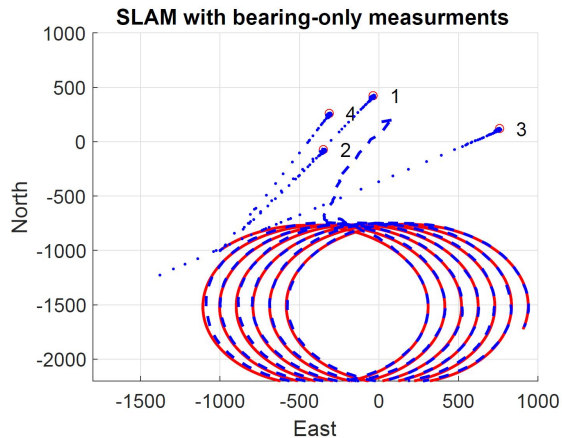


Fig. 3: The landmark and vehicle position estimates of the bearing only SLAM. For this figure, the end position estimate is set equal to the true end position for easier comparison in the figure, and one can see that the evolution of the position estimates converge to the same trajectory as the true vessel.

VII. CONCLUSION

In this article we have presented a globally asymptotically stable bearing only SLAM estimation, that is able to estimate landmarks and its relative position with bearing only measurements in addition to IMU, velocity and attitude measurements. The system was represented as an LTV system, where an observability analysis was performed; in which conditions on the trajectory was found so that with KF, global convergence could be achieved in the nominal case. A new design of the input covariances was proposed, using the Jacobian of the system.

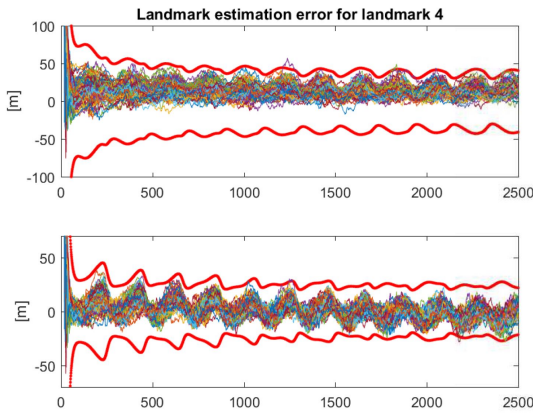


Fig. 4: The error of 150 trajectories of the Landmark 3 estimates, with 3σ plotted red. Here the covariance matrix is the covariance from linearization added with a diagonal matrix. It is apparent that the biased estimates offsets the error.

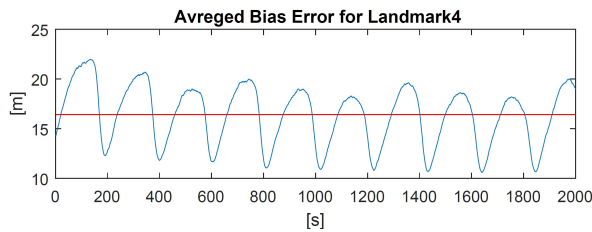


Fig. 5: The mean error in range estimates of landmark 4 from 3000 MC simulations, from $500 < t < 2500$.

A. Future work

Future work include further analysis of the noise characteristics of the bearing only SLAM solution and exploration of the noise correlation structure in detail. In addition, the goal is to develop an attitude observer for bearing only measurements, which is not dependent on magnetometer to estimate gyro bias, and experimental validation of the SLAM solution together with solutions presented in [10].

ACKNOWLEDGEMENT

This work was supported by the Research Council of Norway through the Centres of Excellence funding scheme, project number 250725, and Centre for autonomous marine operations and systems, project number 223254.

REFERENCES

[1] B. J. Guerreiro, P. Batista, C. Silvestre, and P. Oliveira, "Globally asymptotically stable sensor-based simultaneous localization and mapping," *IEEE Transactions on Robotics*, vol. 29, no. 6, pp. 1380–1395, 2013.

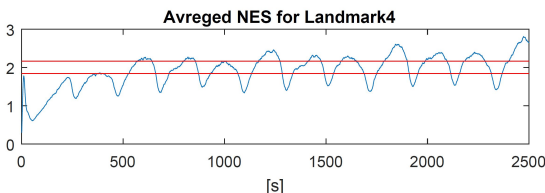


Fig. 6: NES test of Bearing only SLAM with 1000 MC simulations and 1% confidence interval for landmark 4, with only linearised covariance matrix. It is apparent that the NES estimates are optimistic, due to the bias estimates.

[2] H. Durrant-Whyte and T. Bailey, "Simultaneous localization and mapping: part I," *IEEE Robotics & Automation Magazine*, vol. 13, no. 2, pp. 99–110, 2006.

[3] T. Bailey and H. Durrant-Whyte, "Simultaneous localization and mapping (SLAM): Part II," *IEEE Robotics & Automation Magazine*, vol. 13, no. 3, pp. 108–117, 2006.

[4] J. A. Castellanos, J. Neira, and J. D. Tardós, "Limits to the consistency of EKF-based SLAM I," 2004.

[5] N. M. Kwok, G. Dissanayake, and Q. P. Ha, "Bearing-only SLAM using a SPRT based gaussian sum filter," in *Proceedings of ICRA 2005*, pp. 1109–1114, IEEE, 2005.

[6] K. E. Bekris, M. Glick, and L. E. Kavraki, "Evaluation of algorithms for bearing-only SLAM," in *Proceedings of ICRA 2006n*, pp. 1937–1943, IEEE, 2006.

[7] L. Zhao, S. Huang, and G. Dissanayake, "Linear MonoSLAM: A linear approach to large-scale monocular SLAM problems," in *Proceedings of ICRA 2014*, pp. 1517–1523, IEEE, 2014.

[8] A. I. Mourikis and S. I. Roumeliotis, "A multi-state constraint Kalman filter for vision-aided inertial navigation," in *Proceedings of IEEE international conference on robotics and automation*, pp. 3565–3572, IEEE, 2007.

[9] M. Li and A. I. Mourikis, "Optimization-based estimator design for vision-aided inertial navigation: Supplemental materials," 2012.

[10] T. A. Johansen and E. Brekke, "Globally exponentially stable kalman filtering for SLAM with AHRS," in *Proceedings of FUSION 2016*, pp. 909–916, IEEE, 2016.

[11] H. F. Grip, T. I. Fossen, T. A. Johansen, and A. Saberi, "Attitude estimation based on time-varying reference vectors with biased gyro and vector measurements," *IFAC World Congress Proceedings*, vol. 44, no. 1, pp. 8497–8502, 2011.

[12] B. Anderson, "Stability properties of kalman-bucy filters," *Journal of the Franklin Institute*, vol. 291, no. 2, pp. 137–144, 1971.

[13] P. Batista, C. Silvestre, and P. Oliveira, "Single range aided navigation and source localization: Observability and filter design," *Systems & Control Letters*, vol. 60, no. 8, pp. 665–673, 2011.

[14] P. Lourenço, B. J. Guerreiro, P. Batista, P. Oliveira, and C. Silvestre, "3-d inertial trajectory and map online estimation: Building on a GAS sensor-based SLAM filter," in *Proceedings of ECC 2013*, pp. 4214–4219, IEEE, 2013.

[15] J. Sola, "Quaternion kinematics for the error-state KF," *Laboratoire d'Analyse et d'Architecture des Systemes-Centre national de la recherche scientifique (LAAS-CNRS), Toulouse, France, Tech. Rep.*, 2012.

[16] T. I. Fossen, *Handbook of Marine Craft Hydrodynamics and Motion Control*. Wiley, 2011.

[17] T. Kailath, *Linear systems*, vol. 156. Prentice-Hall Englewood Cliffs, NJ, 1980.

[18] L. M. Silverman and B. D. Anderson, "Controllability, observability and stability of linear systems," *SIAM Journal on control*, vol. 6, no. 1, pp. 121–130, 1968.

[19] R. E. Kalman, "Mathematical description of linear dynamical systems," *Journal of the Society for Industrial and Applied Mathematics, Series A: Control*, vol. 1, no. 2, pp. 152–192, 1963.

[20] P. Lourenço, P. Batista, P. Oliveira, C. Silvestre, and C. P. Chen, "Sensor-based globally exponentially stable range-only simultaneous localization and mapping," *Robotics and Autonomous Systems*, vol. 68, pp. 72–85, 2015.

[21] J. J. Dacunha, "Transition matrix and generalized matrix exponential via the peano-baker series," *Journal of Difference Equations and Applications*, vol. 11, no. 15, pp. 1245–1264, 2005.

[22] Y. Bar-Shalom, X. R. Li, and T. Kirubarajan, *Estimation with applications to tracking and navigation: theory algorithms and software*. John Wiley & Sons, 2004.